Acta Cryst E
CRYSTALLOGRAPHIC
COMMUNICATIONS

ISSN 2056-9890

Synthesis, crystal structure and Hirshfeld surface analysis of 1,7-dimethyl-5a,6,11a,12-tetrahydrobenzo[*b*]benzo[5,6][1,4]oxazino[2,3-e][1,4]oxazine

Emine Berrin Çınar,[a] Semanur Yeşilbağ,[b] Onur Erman Doğan,[b] Erbil Ağar,[b] Necmi Dege[a]* and Eiad Saif[c]*

[a]Department of Physics, Faculty of Arts and Sciences, Ondokuz Mayıs University, Samsun, 55200, Turkey, [b]Department of Chemistry, Faculty of Arts and Sciences, Ondokuz Mayıs, University, Samsun, 55200, Turkey, and [c]Department of Computer and Electronic Engineering Technology, Sana'a Community, College, Sana'a, Yemen. *Correspondence e-mail: 'necmisamsun@gmail.com', eiad.saif@scc.edu.ye

Received 1 July 2020
Accepted 2 August 2020

Edited by A. V. Yatsenko, Moscow State University, Russia

Keywords: crystal structure; Hirshfeld surface; DFT; oxazines.

CCDC reference: 2021045

Supporting information: this article has supporting information at journals.iucr.org/e

Molecules of the title compound, $C_{16}H_{16}N_2O_2$, occupy special positions on the twofold rotation axes. The heterocyclic ring adopts a slightly twisted envelope conformation with one of the two junction carbon atoms as the flap. The mean planes through the two halves of the molecule form a dihedral angle of 72.01 (2)°. In the crystal, molecules are linked by pairs of C—H⋯O and N—H⋯C contacts into layers parallel to (100). H⋯H contacts make the largest contribution to the Hirshfeld surface (58.9%).

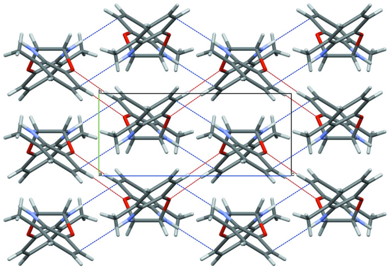

1. Chemical context

The title oxazine derivative contains two six-membered heterocyclic rings located between two benzene rings. Oxazine-derived compounds are used in the synthesis of detergents, corrosion inhibitors and industrial dyes (Adib *et al.*, 2006). This class of molecules has been studied extensively as they exhibit antitumor (Sriharsha *et al.*, 2006), antibacterial and antifungal (Belz *et al.*, 2013) activity. Oxazinooxazines are important heterocyclic precursors in the construction of heteropropellanes with applications in material sciences and medicinal chemistry (Dilmaç *et al.*, 2017). Such heterocycles can be synthesized by several methods (Konstantinova *et al.*, 2020), with the most direct route being the condensation of amino alcohols with either aldehydes or ketones (Hajji *et al.*, 2003). As the amino and hydroxy groups are adjacent, 2-aminophenol readily forms heterocycles. An interesting feature of the reaction is the stereo-selective transformation of glyoxal. We report herein the crystal structure and Hirshfeld surface analysis for a new oxazine derivative, 1,7-dimethyl-5a,6,11a,12-tetrahydrobenzo[*b*]benzo[5,6][1,4]oxazino[2,3-*e*]-[1,4]oxazine.

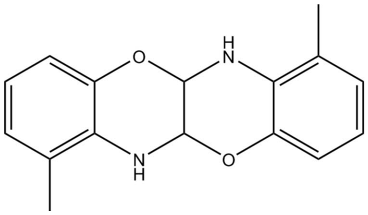

2. Structural commentary

The molecular structure of the title compound (I) is shown in Fig. 1. The molecules occupy special positions on the twofold

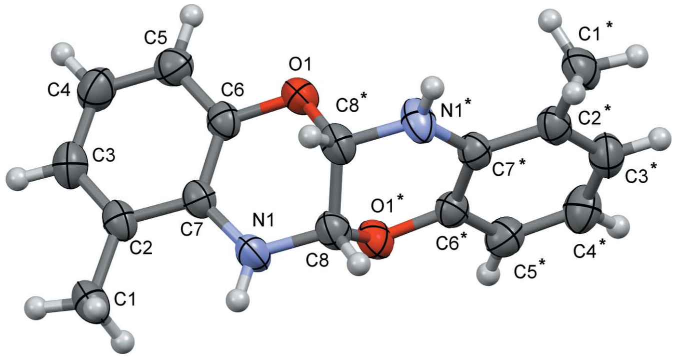

Figure 1
The molecular structure of the title compound, showing the atom labelling and displacement ellipsoids drawn at the 40% probability level. Starred atoms are generated by the symmetry operation $-x - 1, y, -z - \frac{1}{2}$.

rotation axes. The heterocyclic ring adopts a slightly twisted envelope conformation with the C8* [symmetry code: (*) $-x - 1, y, -z - \frac{1}{2}$] atom as the flap. Except for this atom, the symmetry-independent part of the molecule (C2–C8/O1/N1) is nearly planar, the largest separation from the mean plane being 0.1267 (10) Å for O1. The mean planes of the two halves of the molecule form a dihedral angle of 72.01 (2)°.

3. Supramolecular features

Surprisingly, no intermolecular N—H$\cdots$O contacts are observed in the title structure. Instead, C—H$\cdots$O and N—H$\cdots$C contacts are formed, the latter really being of the N—H$\cdots\pi$ type. Pairs of C—H$\cdots$O contacts link the molecules into zigzag chains along [001] (Table 1, Fig. 2). Pairs of N—H$\cdots$O contacts also form zigzag chains of molecules along [001] (Table 1, Fig. 3). As a result, layers parallel to (100) are formed (Fig. 4).

Table 1
Hydrogen-bond geometry (Å, °).

D—H$\cdots A$	D—H	H$\cdots A$	$D\cdots A$	D—H$\cdots A$
C5—H5$\cdots$O1$^{\rm i}$	0.93	2.59	3.513 (2)	172
N1—H1$\cdots$C5$^{\rm ii}$	0.86	2.64	3.375 (2)	144

Symmetry codes: (i) $-x - 1, -y + 2, -z$; (ii) $x, -y + 1, z - \frac{1}{2}$.

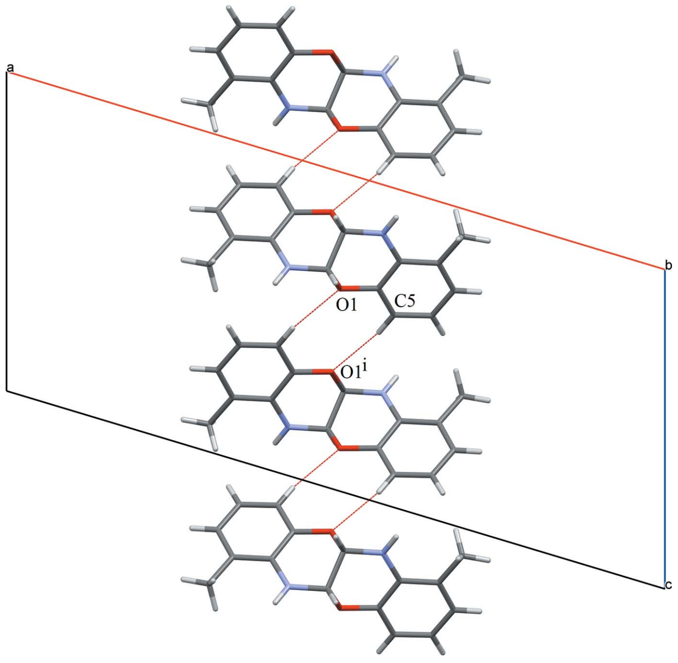

Figure 2
Chains of the title molecules linked by pairs of C—H$\cdots$O interactions.

4. Hirshfeld surface

The Hirshfeld surfaces were generated using *Crystal Explorer 17.5* (Turner *et al.*, 2017). The $d_{\rm norm}$ mapping was performed in the range of −0.186 to 1.019 arbitrary units. Red spots on the $d_{\rm norm}$ surface (Fig. 5) indicate regions of C—H$\cdots$O interactions. However, the N—H$\cdots$C contacts do not cause red

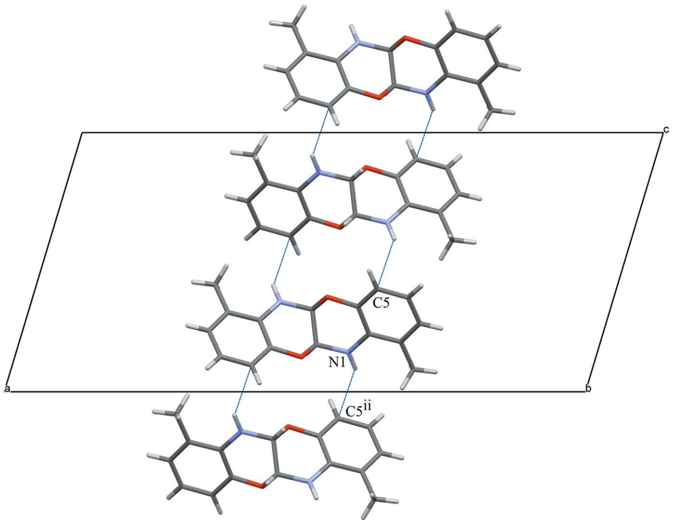

Figure 3
Chains of molecules linked by pairs of N—H$\cdots$C interactions.

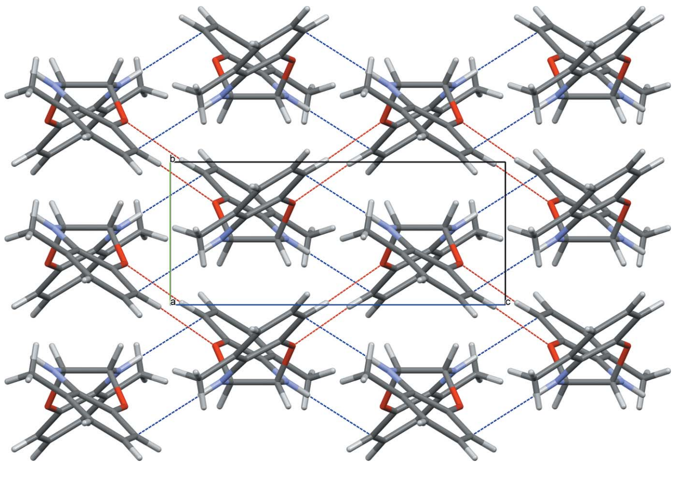

Figure 4
Layer of the title molecules linked by C—H$\cdots$O (red) and N—H$\cdots$C (blue) interactions.

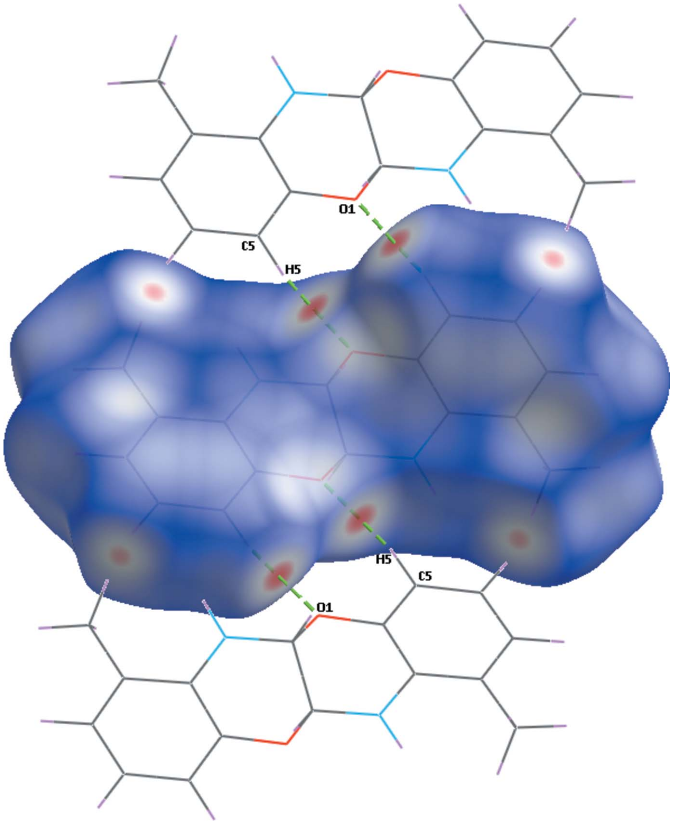

Figure 5
View of the three-dimensional Hirshfeld surface for the title molecule plotted over $d_{\rm norm}$.

spots on the Hirshfeld surface. Other red spots are due to the H···H interactions, as can be understood from the fingerprint plot. The characteristic flat surface patches caused by planar stacking are shown in Fig. 6*a*. The shape-index map (Fig. 6*b*) does not contain red and blue triangles related to π–π interactions. Fig. 6*c*,*d* show the d_i and d_e surfaces, respectively. Fig. 7 presents the two-dimensional fingerprint plot for the title molecule and those delineated into the specific types of interactions. The H···H contacts make the largest contribution to the Hirshfeld surface (58.9%). The H···C/C···H interactions are seen at the edges of two-dimensional fingerprint drawings, with a general contribution of 24.6%.

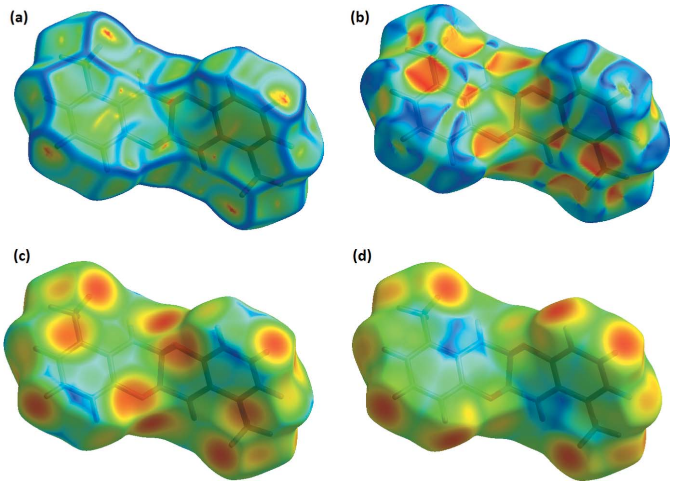

Figure 6
The Hirshfeld surfaces of the title molecule mapped over (*a*) curvedness, (*b*) shape-index, (*c*) d_i and (*d*) d_e.

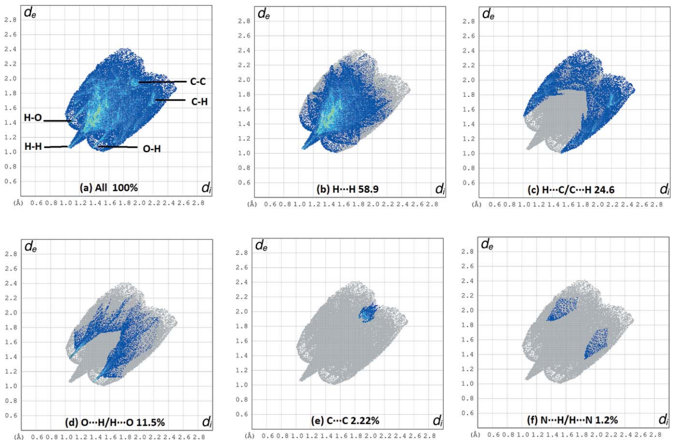

Figure 7
Two-dimensional fingerprint plot for the title molecule (*a*) and those delineated into the specific types of interactions (*b*–*f*).

5. Database survey

A search of the Cambridge Structural Database (CSD, version 5.40, update of August 2019; Groom *et al.*, 2016) using 1-benzyl-3,4-dihydroquinoxalin-2(1*H*)-one as the main skeleton revealed the presence of four structures similar to the title compound. These are 2,8-di-*t*-butyl-5a,6,11a,12-tetrahydro[1,4]benzoxazino[3,672-*b*][1,4]benzoxazine (MOYJOC; Niklas *et al.*, 2019), 5a,6,11a,12-tetrahydro[1,4]benzoxazino[3,2-*b*][1,4]benzoxazine (FIGVOG; Tauer *et al.*, 1986), 5a,6,11a,12-tetrahydro-5a,11a-dimethyl-1,4-benzoxazino[3,2-*b*][1,4]benzoxazine (ABEQAA; Hai-Yan *et al.*, 2004) and *N*,*N*′-di-5a,6,11a,12-tetrahydro[1,4]benzoxazino[3,2]benzoxazine (BAJNIJ; Farfán *et al.*, 1992). In the structures MOYJOC and FIGVOG, the dihedral angles between the two approximately planar halves of the molecule [67.11 (3) and 64.28 (2)°, respectively] are smaller than in (I). In MOYJOC, both NH groups are involved in hydrogen bonds with the heterocyclic oxygen atoms. In FIGVOG, only one NH group takes part in such hydrogen bonding, while the other makes an N—H···C contact similar to that observed in (I). In ABEQAA, the hydrogen atoms at the bridge C atoms (C8 and C8* in the title molecule) are replaced by methyl groups. As a result, the dihedral angle increases to 81.70 (2)°. In this structure, both NH groups form weak intermolecular N—H···O hydrogen bonds.

6. Synthesis and crystallization

To a solution of 2-amino-3-methylphenol (21.8 mg, 0.177 mmol) in ethanol (20 ml), was added glyoxal (40 wt % solution in H_2O) (12.8 mg, 0.089 mmol) dissolved in ethanol

(20 ml) and the mixture was refluxed for 12 h. The orange product obtained was washed with ether and recrystallized from ethanol at room temperature (m.p. 472-475 K, yield 67%).

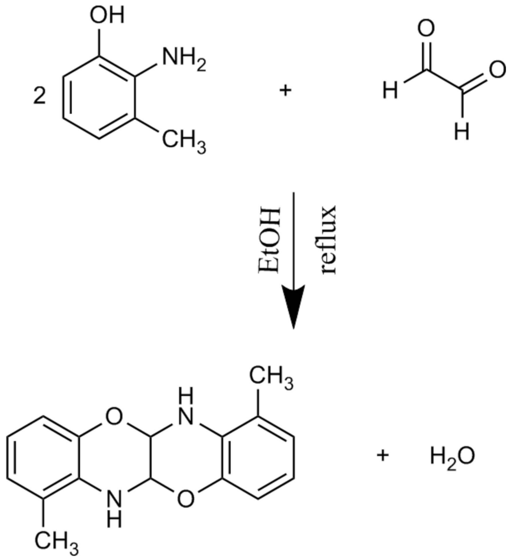

7. Refinement

Crystal data, data collection and structure refinement details are summarized in Table 2. All hydrogen atoms were constrained to ride on their parent atoms with C—H = 0.93, 0.96 and 0.98 Å for aromatic, methyl and methine H atoms, respectively, and with N—H = 0.86 Å. Isotropic displacement parameters of these atoms were constrained to $1.5U_{\rm eq}$(C) for the methyl group and to $1.2U_{\rm eq}$(C,N) for all other H atoms.

Table 2
Experimental details.

Crystal data	
Chemical formula	$C_{16}H_{16}N_2O_2$
M_r	268.31
Crystal system, space group	Monoclinic, *C*2/*c*
Temperature (K)	296
a, *b*, *c* (Å)	24.798 (3), 4.7133 (4), 11.5330 (14)
β (°)	106.751 (9)
V (Å^3)	1290.8 (3)
Z	4
Radiation type	Mo *Kα*
μ (mm^{-1})	0.09
Crystal size (mm)	0.78 × 0.42 × 0.13
Data collection	
Diffractometer	Stoe IPDS 2
Absorption correction	Integration (*X-RED32*; Stoe & Cie, 2002)
$T_{\rm min}$, $T_{\rm max}$	0.941, 0.989
No. of measured, independent and observed [$I > 2\sigma(I)$] reflections	5580, 2194, 1024
$R_{\rm int}$	0.059
$(\sin \theta/\lambda)_{\rm max}$ (Å^{-1})	0.745
Refinement	
$R[F^2 > 2\sigma(F^2)]$, $wR(F^2)$, S	0.049, 0.134, 0.88
No. of reflections	2194
No. of parameters	92
H-atom treatment	H-atom parameters constrained
$\Delta\rho_{\rm max}$, $\Delta\rho_{\rm min}$ (e Å^{-3})	0.15, −0.16

Computer programs: *X-AREA* and *X-RED32* (Stoe & Cie, 2002), *SHELXT2018/3* (Sheldrick, 2015*a*), *SHELXL2018/3* (Sheldrick, 2015*b*), *OLEX2* (Dolomanov *et al.*, 2009), *Mercury* (Macrae *et al.*, 2020), *WinGX* (Farrugia, 2012), *PLATON* (Spek, 2020) and *publCIF* (Westrip, 2010).

Acknowledgements

The authors acknowledge the Faculty of Arts and Sciences, Ondokuz Mayıs University, Turkey, for the use of the Stoe IPDS 2 diffractometer (purchased under grant F.279 of the University Research Fund).

References

Adib, M., Sheibani, E., Mostofi, M., Ghanbary, K. & Bijanzadeh, H. R. (2006). *Tetrahedron*, **62**, 3435–3438.
Belz, T., Ihmaid, S., Al-Rawi, J. & Petrovski, S. (2013). *Int. J. Med. Chem.* Article ID 436397.
Dilmaç, M., Spuling, E., de Meijere, A. & Bräse, S. (2017). *Angew. Chem. Int. Ed.* **56**, 5684–5718.
Dolomanov, O. V., Bourhis, L. J., Gildea, R. J., Howard, J. A. K. & Puschmann, H. (2009). *J. Appl. Cryst.* **42**, 339–341.
Farfán, N., Santillan, R. L., Castillo, D., Cruz, R., Joseph-Nathan, P. & Daran, J. (1992). *Can. J. Chem.* **70**, 2764–2770.
Farrugia, L. J. (2012). *J. Appl. Cryst.* **45**, 849–854.
Groom, C. R., Bruno, I. J., Lightfoot, M. P. & Ward, S. C. (2016). *Acta Cryst.* B**72**, 171–179.
Hai-Yan, Z., Xiao-Hang, Q. & Pan-Wen, S. (2004). *Acta Cryst.* E**60**, o1619–o1621.
Hajji, C., Zaballos-García, E. & Sepúlveda-Arques, J. (2003). *Synth. Commun.* **33**, 4347–4354.
Konstantinova, L. S., Tolmachev, M. A., Popov, V. V. & Rakitin, O. A. (2020). *Molbank*, Article M1149.
Macrae, C. F., Sovago, I., Cottrell, S. J., Galek, P. T. A., McCabe, P., Pidcock, E., Platings, M., Shields, G. P., Stevens, J. S., Towler, M. & Wood, P. A. (2020). *J. Appl. Cryst.* **53**, 226–235.
Niklas, J. E., Hunter, H. M. & Gorden, A. E. V. (2019). *Inorg. Chem.* **58**, 15088–15100.
Sheldrick, G. M. (2015*a*). *Acta Cryst.* A**71**, 3–8.
Sheldrick, G. M. (2015*b*). *Acta Cryst.* C**71**, 3–8.
Spek, A. L. (2020). *Acta Cryst.* E**76**, 1–11.
Sriharsha, S. & Shashikanth, S. (2006). *Heterocycl. Commun.* **12**, 213–218.
Stoe & Cie (2002). *X-AREA* and *X-RED32*. Stoe & Cie, Darmstadt, Germany.
Tauer, E., Grellmann, K. H., Kaufmann, E. & Noltemeyer, M. (1986). *Chem. Ber.* **119**, 3316–3325.
Turner, M. J., MacKinnon, J. J., Wolff, S. K., Grimwood, D. J., Spackman, P. R., Jayatilaka, D. & Spackman, M. A. (2017). *Crystal Explorer 17.5*. University of Western Australia.
Westrip, S. P. (2010). *J. Appl. Cryst.* **43**, 920–925.

supporting information

Acta Cryst. (2020). E**76**, 1472-1475 [https://doi.org/10.1107/S2056989020010646]

Synthesis, crystal structure and Hirshfeld surface analysis of 1,7-dimethyl-5a,6,11a,12-tetrahydrobenzo[*b*]benzo[5,6][1,4]oxazino[2,3-e][1,4]oxazine

Emine Berrin Çınar, Semanur Yeşilbağ, Onur Erman Doğan, Erbil Ağar, Necmi Dege and Eiad Saif

Computing details

Data collection: *X-AREA* (Stoe & Cie, 2002); cell refinement: *X-AREA* (Stoe & Cie, 2002); data reduction: *X-RED32* (Stoe & Cie, 2002); program(s) used to solve structure: *SHELXT2018/3* (Sheldrick, 2015a); program(s) used to refine structure: *SHELXL2018/3* (Sheldrick, 2015b); molecular graphics: *OLEX2* (Dolomanov *et al.*, 2009) and *Mercury* (Macrae *et al.*, 2020); software used to prepare material for publication: *WinGX* (Farrugia, 2012), *SHELXL2018/3* (Sheldrick, 2015b), *PLATON* (Spek, 2020) and *publCIF* (Westrip, 2010).

1,7-Dimethyl-5a,6,11a,12-tetrahydrobenzo[*b*]benzo[5,6][1,4]oxazino[2,3-e][1,4]oxazine

Crystal data

$C_{16}H_{16}N_2O_2$	D_x = 1.381 Mg m^{-3}
M_r = 268.31	Melting point = 472–475 K
Monoclinic, $C2/c$	Mo $K\alpha$ radiation, λ = 0.71073 Å
a = 24.798 (3) Å	Cell parameters from 3858 reflections
b = 4.7133 (4) Å	θ = 1.8–32.0°
c = 11.5330 (14) Å	μ = 0.09 mm^{-1}
β = 106.751 (9)°	T = 296 K
V = 1290.8 (3) Å^3	Plate, orange
Z = 4	0.78 × 0.42 × 0.13 mm
F(000) = 568	

Data collection

Stoe IPDS 2 diffractometer	T_{min} = 0.941, T_{max} = 0.989
Radiation source: sealed X-ray tube, 12 x 0.4 mm long-fine focus′	5580 measured reflections
Plane graphite monochromator	2194 independent reflections
Detector resolution: 6.67 pixels mm^{-1}	1024 reflections with $I > 2\sigma(I)$
rotation method scans	R_{int} = 0.059
Absorption correction: integration (X-RED32; Stoe & Cie, 2002)	θ_{max} = 32.0°, θ_{min} = 3.4°
	h = −35→36
	k = −7→6
	l = −16→16

Refinement

Refinement on F^2
Least-squares matrix: full
$R[F^2 > 2\sigma(F^2)] = 0.049$
$wR(F^2) = 0.134$
$S = 0.88$
2194 reflections
92 parameters
0 restraints
Primary atom site location: structure-invariant direct methods
Secondary atom site location: difference Fourier map
Hydrogen site location: inferred from neighbouring sites
H-atom parameters constrained
$w = 1/[\sigma^2(F_o^2) + (0.0639P)^2]$ where $P = (F_o^2 + 2F_c^2)/3$
$(\Delta/\sigma)_{max} < 0.001$
$\Delta\rho_{max} = 0.15$ e Å^{-3}
$\Delta\rho_{min} = -0.16$ e Å^{-3}

Special details

Geometry. All esds (except the esd in the dihedral angle between two l.s. planes) are estimated using the full covariance matrix. The cell esds are taken into account individually in the estimation of esds in distances, angles and torsion angles; correlations between esds in cell parameters are only used when they are defined by crystal symmetry. An approximate (isotropic) treatment of cell esds is used for estimating esds involving l.s. planes.

Fractional atomic coordinates and isotropic or equivalent isotropic displacement parameters (Å^2)

	x	*y*	*z*	U_{iso}*/U_{eq}
O1	−0.50672 (4)	0.7122 (2)	−0.13429 (9)	0.0582 (3)
N1	−0.57174 (5)	0.4629 (3)	−0.34733 (13)	0.0622 (4)
H1	−0.591648	0.369876	−0.409012	0.075*
C7	−0.59760 (6)	0.6173 (3)	−0.27650 (13)	0.0484 (3)
C2	−0.65643 (6)	0.6435 (3)	−0.30692 (14)	0.0531 (4)
C6	−0.56462 (6)	0.7472 (3)	−0.17100 (13)	0.0497 (3)
C8	−0.51247 (6)	0.4590 (3)	−0.31772 (14)	0.0545 (4)
H8	−0.500090	0.289696	−0.352275	0.065*
C3	−0.67936 (7)	0.8104 (4)	−0.23575 (17)	0.0657 (5)
H3	−0.718296	0.828025	−0.255126	0.079*
C5	−0.58834 (7)	0.9190 (3)	−0.10285 (15)	0.0599 (4)
H5	−0.565754	1.011706	−0.034970	0.072*
C1	−0.69244 (7)	0.4830 (4)	−0.41332 (17)	0.0675 (5)
H1A	−0.682704	0.536853	−0.485013	0.101*
H1B	−0.731357	0.526107	−0.423392	0.101*
H1C	−0.686334	0.283070	−0.399720	0.101*
C4	−0.64605 (8)	0.9525 (4)	−0.13620 (18)	0.0709 (5)
H4	−0.662501	1.070905	−0.091513	0.085*

Atomic displacement parameters (Å^2)

	U^{11}	U^{22}	U^{33}	U^{12}	U^{13}	U^{23}
O1	0.0456 (6)	0.0679 (7)	0.0562 (6)	−0.0052 (4)	0.0068 (5)	−0.0074 (5)
N1	0.0411 (7)	0.0735 (8)	0.0664 (8)	−0.0036 (6)	0.0067 (6)	−0.0223 (7)
C7	0.0436 (7)	0.0457 (7)	0.0545 (8)	−0.0027 (6)	0.0122 (6)	0.0014 (6)
C2	0.0435 (7)	0.0526 (8)	0.0612 (9)	−0.0031 (6)	0.0120 (7)	0.0087 (7)
C6	0.0449 (7)	0.0509 (7)	0.0534 (8)	−0.0046 (6)	0.0146 (6)	0.0049 (7)
C8	0.0429 (7)	0.0554 (8)	0.0621 (9)	0.0023 (6)	0.0101 (7)	−0.0047 (7)
C3	0.0487 (9)	0.0707 (10)	0.0806 (12)	0.0037 (8)	0.0234 (9)	0.0044 (9)

C5	0.0648 (10)	0.0610 (9)	0.0565 (9)	−0.0076 (7)	0.0214 (7)	−0.0040 (7)
C1	0.0450 (8)	0.0771 (10)	0.0726 (11)	−0.0070 (7)	0.0044 (7)	0.0036 (9)
C4	0.0669 (11)	0.0733 (11)	0.0811 (12)	0.0031 (8)	0.0349 (10)	−0.0104 (10)

Geometric parameters (Å, º)

O1—C6	1.3846 (17)	C8—C8^{i}	1.505 (3)
O1—C8^{i}	1.4521 (18)	C8—H8	0.9800
N1—C7	1.3822 (19)	C3—C4	1.379 (3)
N1—C8	1.4099 (19)	C3—H3	0.9300
N1—H1	0.8600	C5—C4	1.380 (2)
C7—C6	1.397 (2)	C5—H5	0.9300
C7—C2	1.4041 (19)	C1—H1A	0.9600
C2—C3	1.373 (2)	C1—H1B	0.9600
C2—C1	1.498 (2)	C1—H1C	0.9600
C6—C5	1.373 (2)	C4—H4	0.9300
C6—O1—C8^{i}	113.95 (11)	O1^{i}—C8—H8	109.8
C7—N1—C8	119.51 (12)	C8^{i}—C8—H8	109.8
C7—N1—H1	120.2	C2—C3—C4	121.60 (15)
C8—N1—H1	120.2	C2—C3—H3	119.2
N1—C7—C6	119.38 (12)	C4—C3—H3	119.2
N1—C7—C2	121.63 (14)	C6—C5—C4	119.27 (16)
C6—C7—C2	118.98 (14)	C6—C5—H5	120.4
C3—C2—C7	118.72 (15)	C4—C5—H5	120.4
C3—C2—C1	121.82 (14)	C2—C1—H1A	109.5
C7—C2—C1	119.43 (15)	C2—C1—H1B	109.5
C5—C6—O1	118.20 (13)	H1A—C1—H1B	109.5
C5—C6—C7	121.14 (13)	C2—C1—H1C	109.5
O1—C6—C7	120.64 (12)	H1A—C1—H1C	109.5
N1—C8—O1^{i}	109.28 (12)	H1B—C1—H1C	109.5
N1—C8—C8^{i}	109.82 (15)	C3—C4—C5	120.05 (16)
O1^{i}—C8—C8^{i}	108.29 (9)	C3—C4—H4	120.0
N1—C8—H8	109.8	C5—C4—H4	120.0
C8—N1—C7—C6	−5.4 (2)	N1—C7—C6—O1	−2.8 (2)
C8—N1—C7—C2	175.60 (14)	C2—C7—C6—O1	176.19 (13)
N1—C7—C2—C3	−177.10 (14)	C7—N1—C8—O1^{i}	−82.21 (17)
C6—C7—C2—C3	3.9 (2)	C7—N1—C8—C8^{i}	36.44 (15)
N1—C7—C2—C1	4.7 (2)	C7—C2—C3—C4	0.3 (2)
C6—C7—C2—C1	−174.29 (14)	C1—C2—C3—C4	178.44 (16)
C8^{i}—O1—C6—C5	159.07 (13)	O1—C6—C5—C4	−178.67 (14)
C8^{i}—O1—C6—C7	−22.75 (17)	C7—C6—C5—C4	3.2 (2)
N1—C7—C6—C5	175.29 (14)	C2—C3—C4—C5	−2.9 (3)
C2—C7—C6—C5	−5.7 (2)	C6—C5—C4—C3	1.1 (2)

Symmetry code: (i) $-x-1, y, -z-1/2$.

Hydrogen-bond geometry (Å, º)

D—H···*A*	*D*—H	H···*A*	*D*···*A*	*D*—H···*A*
C5—H5···O1^{ii}	0.93	2.59	3.513 (2)	172
N1—H1···C5^{iii}	0.86	2.64	3.375 (2)	144

Symmetry codes: (ii) −*x*−1, −*y*+2, −*z*; (iii) *x*, −*y*+1, *z*−1/2.

Selected bond lengths, bond and dihedral angles (° A, °) in the title structure

Parameters	Å, °
O1—C6	1.3846 (17)
O1—C8*	1.4521 (18)
N1—C8	1.4099 (19)
N1—C7	1.3822 (19)
C8—C8*	1.505 (3)
C6—C7	1.397 (2)
O1*—C8—C8*	108.29 (9)
N1—C8—C8*	109.82 (15)
N1—C8—O1*	109.28 (12)
C6—O1—C8*	113.95 (11)
C7—N1—C8—C8*	36.44 (15)
C8*—O1—C6—C7	-22.75 (17)
C2—C7—C6—C5	-5.7 (2)
N1—C7—C6—O1	-2.8 (2)